Article

ACS AuthorChoice

Interleukin-10: An Anti-Inflammatory Marker To Target Atherosclerotic Lesions via PEGylated Liposomes

Gunter Almer,[†,‡,§] Daniela Frascione,[†,§] Isabella Pali-Schöll,[ǁ] Caroline Vonach,[†] Anna Lukschal,[⊥] Caroline Stremnitzer,[⊥] Susanne C. Diesner,[#] Erika Jensen-Jarolim,[ǁ,⊥] Ruth Prassl,[¶,○] and Harald Mangge*,[‡]

[†]Institute of Biophysics and Nanosystems Research, Austrian Academy of Science, Graz, Austria

[ǁ]Messerli Research Institute of the University of Veterinary Medicine Vienna, Medical University of Vienna, University of Vienna, Austria

[⊥]Department of Pathophysiology and Allergy Research, Medical University of Vienna, Austria

[¶]Institute of Biophysics, Medical University of Graz, Austria

[○]Ludwig Boltzmann Institute for Lung Vascular Research, Graz, Austria

[#]Department of Pediatrics and Adolescent Medicine, Medical University of Vienna, Austria

[‡]Clinical Institute of Medical and Chemical Laboratory Diagnostics—Research Unit on Lifestyle and Inflammation-Associated Risk Biomarkers, Medical University of Graz, Austria

S *Supporting Information*

ABSTRACT: Atherosclerosis (AS) causes cardiovascular disease, which leads to fatal clinical end points like myocardial infarction or stroke, the most prevalent causes of death in developed countries. An early, noninvasive method of detection and diagnosis of atherosclerotic lesions is necessary to prevent and treat these clinical end points. Working toward this goal, we examined recombinant interleukin-10 (IL-10), stealth liposomes with nano-cargo potency for NMRI relevant contrast agents, and IL-10 coupled to stealth liposomes in an ApoE-deficient mouse model using confocal laser-scanning microscopy (CLSM). Through *ex vivo* incubation and imaging with CLSM, we showed that fluorescently labeled IL-10 is internalized by AS plaques, and a low signal is detected in both the less injured aortic surfaces and the arteries of wild-type mice. *In vivo* experiments included intravenous injections of (i) fluorescent IL-10, (ii) IL-10 targeted carboxyfluorescin (CF−) labeled stealth liposomes, and (iii) untargeted CF-labeled stealth liposomes. Twenty-four hours after injection the arteries were dissected and imaged *ex vivo*. Compared to free IL-10, we observed a markedly stronger fluorescence intensity with IL-10 targeted liposomes at AS plaque regions. Moreover, untargeted CF-labeled liposomes showed only weak, unspecific binding. Neither free IL-10 nor IL-10 targeted liposomes showed significant immune reaction when injected into wild-type mice. Thus, the combined use of specific anti-inflammatory proteins, high payloads of contrast agents, and liposome particles should enable current imaging techniques to better recognize and visualize AS plaques for research and prospective therapeutic strategies.

KEYWORDS: IL-10, liposomes, atherosclerosis, inflammation, imaging
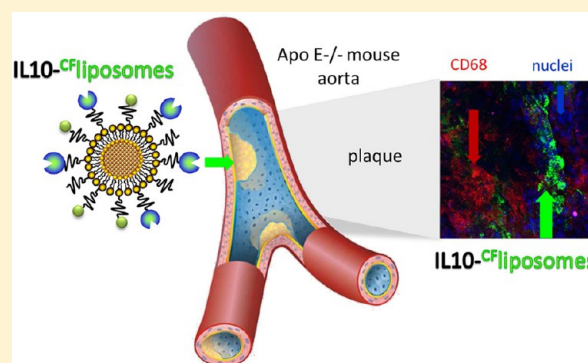
INTRODUCTION

Despite considerable therapeutic advances over the past 50 years, cardiovascular events are the leading causes of death worldwide. This is primarily due to the increasing prevalence of atherosclerosis (AS). AS is recognized as a subacute inflammatory condition of the aortic vessel wall, characterized by the infiltration of macrophages and T-cells which interact with one another and with the arterial wall cells.[1] Currently, AS can only be diagnosed at the advanced stages of the disease: either by directly measuring the degree of stenosis or by evaluating the effect of arterial stenosis on organ perfusion.[2]

Over the past few years, advances have been made in imaging techniques that enable the visualization and monitoring of AS lesions' progression or regression.[3] However, a reliable, noninvasive technique to detect different stages of AS for an applicable, clinical characterization of AS plaques has still not been developed.[4]

In the course of inflammation, various cytokines have been reported to stimulate the progression of AS,[5] whereas few were found to potentially aid in AS regression. Interleukin-10 (IL-10),[6,7] the most prominent anti-inflammatory cytokine, belongs to the type II cytokines.[8] In contrast to most of the other interleukins, IL-10 is primarily known for its role in suppressing immune and inflammatory responses by inhibiting the production of pro-inflammatory cytokines and mediators from macrophages and dendritic cells.[9−11]

Many cells are now known to produce IL-10. Major sources are T-helper cells[12] such as CD8 positive T-cells,[13] monocytes and appropriately stimulated macrophages,[9] and several subsets of dendritic cells;[10] human B cells;[14] eosinophilic granulocytes and mast cells;[15] and some nonimmune cell sources like keratinocytes, epithelial cells, and tumor cells.[16,17]

Recombinant IL-10 has already been used in humans for therapeutic interventions.[18] A study by Chernoff et al. showed that IL-10 is well tolerated without serious side effects at doses up to 25 μg/kg, while mild to moderate flulike symptoms were observed in a fraction of recipients at doses up to 100 μg/kg.[16] It has also been shown that treatment with IL-10 inhibits the development of type I diabetes mellitus in nonobese diabetic (NOD) mice.[19]

It is currently understood that IL-10 signals through a two-receptor complex: IL-10 receptor 1 (IL-10R1) and IL-10 receptor 2 (IL-10R2).[20] Most hematopoietic cells and non-hematopoietic cells, such as fibroblasts and epithelial cells, constitutively express low levels of IL-10R1 and IL-10R2.[21−23] This receptor expression can then be dramatically upregulated by various stimuli. Summarized, the IL-10-binding receptor complex is one of only a few regulating factors known so far. Moreover, numerous, diverse cells have the ability to bind to and consume IL-10. Therefore, IL-10 is an attractive protein as a potential diagnostic marker for AS, and it now needs to be specifically characterized in the AS scenario.

Targeted probes tested for cardiovascular imaging typically include a moiety linked to a specific nanoparticle (NP) which is fused to a contrast agent appropriate to the applied imaging technique.[24,25] The moiety, such as an antibody, biomarker, or specific ligand, has a high affinity for the desired target molecule. Liposomes, vesicles composed of a lipid bilayer, are prominent among the NPs in use. The surface of liposomes is often coated with polyethylene glycol (PEG) molecules to yield "stealth" particles which can elude the reticuloendothelial system (RES) and, thus, have extended circulation times from hours to days.[26] Such liposomes can be easily modified with signal-emitting groups so they may be detected by different imaging modalities. Additionally, functionalized groups can be attached to the distal end of the PEG chains for coupling of specific antibodies or proteins, achieving target recognition by specific cells.[27−29]

In the present study, recombinant IL-10 was explored for the first time as a potential targeting molecule to detect AS lesions. To improve the stability and performance of IL-10 for *in vivo* administration, the protein was coupled to stealth liposomes which also serve as signal-emitting entities.

■ EXPERIMENTAL SECTION

Reagents. Recombinant mouse IL-10 (GenScript, Inc., Piscataway, NJ, USA) and recombinant mouse adiponectin (gAd) (AtgenGlobal, Korea) were both expressed in *Escherichia coli*. Atto655 (ATTO-TEC GmbH, Siegen, Germany), was used either as an amine-reactive carboxylic acid succinimidyl

ester (Atto655-NHS) or as a maleimide-functionalized label (Atto655-Mal).

AlexaFluor (AF) 488 prelabeled rat anti-mouse CD68, AF405 prelabeled rat anti-mouse CD4, and AF488 prelabeled rat anti-mouse CD31 antibodies were purchased from AbDSerotec (Dusseldorf, Germany). A rat, anti-mouse IL-10R antibody and an AF488 prelabeled rat isotype control antibody were purchased from Biozym (Vienna, Austria). A Lightning-Link Atto488 antibody labeling kit was purchased from THP Medical Products (Vienna, Austria).

Lipids used for the synthesis of sterically stabilized PEGylated liposomes were 1-palmitoyl-2-oleoyl-*sn*-glycero-3-phosphocholine (POPC), 1,2-distearoyl-*sn*-glycero-3-phosphoethanolamine-N-[methoxy (polyethylene glycol)-2000] (DSPE-PEG-2000), cholesterol (CH), and 1,2-dioleoyl-*sn*-glycero-3-phosphoethanolamine-N-(carboxyfluorescein) (ammonium salt) (DOPE-CF), all purchased from Avanti Polar Lipids, Inc. (Alabaster, AL, USA), while the functionalized lipid 3-(N-succinimidyloxyglutaryl) aminopropyl, polyethylene glycol-carbamyldistearoylphosphatidyl-ethanolamine (DSPE-PEG-NHS, PEG-chain MW = 2000) was obtained from NOF America Corporation (White Plains, NY, USA). The phospholipid assay kit was purchased from Rolf Greiner BioChemica GmbH (Vienna, Austria).

Fluorescence Labeling. Recombinant IL-10 was labeled as a target molecule using a single, glycosylated polypeptide chain of 161 amino acids (19 kDa, purity >98.0%). The labeling was performed via N-Hydroxysuccinimide (NHS) ester binding using Atto655-NHS, a long wavelength red-emitting fluorescence dye, and in accordance with the standard protocols recommended by the supplier. Briefly, IL-10 was dissolved in 150 mM bicarbonate buffer, pH 8.3, to a final concentration of 1 mg/mL and incubated with a 2-fold molar excess of amine-reactive Atto655-NHS dye, dissolved in dimethyl sulfoxide at a concentration of 2 mg/mL. The Atto655-labeled protein was identified by SDS−PAGE and Western blot analysis (for details see Supporting Information, Figure S1). For comparative staining experiments, recombinant gAd was used as a targeting molecule, which is similar in size (17 kDa) to IL-10. gAd labeling was performed by coupling Atto655-Mal to the single cysteine residue of gAd using a 20-fold molar excess of the dye under basic conditions in phosphate-buffered saline (PBS, 10 mM, 150 mM NaCl, pH 8.0), as described previously.[30] All labeling procedures were carried out at room temperature and followed by extensive dialysis against PBS, pH 7.4 at 4 °C. Dialysis was performed in microdialysis tubes with a molecular weight cutoff of 5 or 10 kDa. The rat, anti-mouse IL-10R antibody was labeled with the Lightning-Link Atto488 antibody labeling kit, following the kit protocol.

Synthesis of IL-10-Targeted PEGylated Liposomes. Sterically stabilized PEGylated liposomes were synthesized using the dry lipid film rehydration method. Briefly, a mixture of lipids consisting of POPC/CH/DSPE-PEG-2000/DOPE-CF/(optionally, DSPE-PEG-NHS) at a molar ratio of 3/2/0.15/0.02/(0.02) was dissolved in organic solvent (chloroform:methanol = 2:1 v/v) in a round-bottom flask, then dried under a stream of nitrogen and left overnight in a vacuum chamber to form a dry lipid film. Functionalized liposomes were prepared by rehydration of the film with 1 mL of 150 mM bicarbonate buffer at pH 8.3 to ensure an efficient reaction with IL-10, while control liposomes (nontargeted PEGylated liposomes consisting of POPC/CH/DSPE-PEG2000 at a molar ratio of 3/2/0.15) were prepared by resuspending the
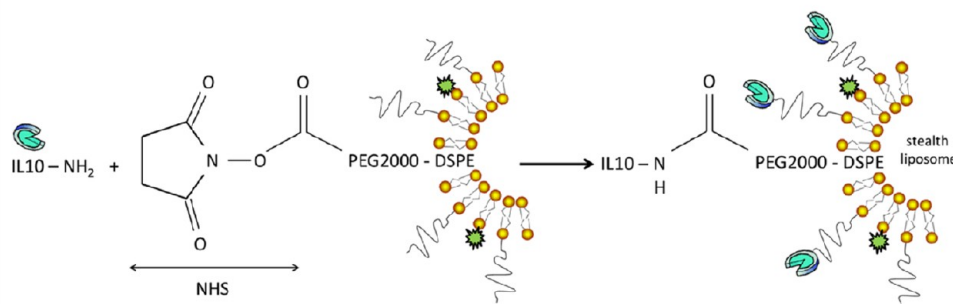
Figure 1. Coupling reaction of IL-10 to liposomes. Recombinant IL-10 was coupled to PEGylated stealth liposomes *via* amine-reactive carboxylic acid succinimidyl (NHS) ester binding. The unbound protein was removed by dialysis.

lipid film in 1 mL of HEPES buffer (20 mM HEPES, 150 mM NaCl and pH 7.4). The final phospholipid concentration of all preparations was 10 mg/mL. During rehydration, the particles were held for one hour at 40 °C and intermittently vortexed to completely resuspend the lipid films. The size of the liposomes was adjusted by extrusion through 200 nm polycarbonate membrane filters (Millipore, Vienna, Austria) using a LiposoFast pneumatic extruder (Avestin Inc., ON, Canada). A schematic description of the procedure is given in the Supporting Information, Figure S2.

The lyophilized IL-10 was dissolved in sterile 18 MΩ-cm water to a final concentration of 0.5 mg/mL, as recommended by the supplier, and an aliquot was added to the extruded liposomes at an NHS to IL-10 molar ratio of 100:1. The coupling reaction was performed overnight at room temperature under constant, slow agitation, and the reaction was stopped by adding a 10-fold molar excess of 2-aminoethanol with respect to NHS. Subsequently, the blocking reagent and the unbound protein were removed by extensive dialysis against HEPES buffer. The molecular weight cutoff of the dialysis membrane is 50 kDa. Figure 1 illustrates the coupling reaction. The protein concentration was determined with a Starcher assay.[31] The binding efficiency of IL-10 to the lipid was roughly quantified by counting the number of IL-10 molecules per liposomes, taking into account a theoretical number of lipids per liposome. The calculations were based on a liposome size of 184 nm on average and a surface area per phospholipid molecule of 0.65 nm^2, as described in more detail in the Supporting Information.

Characterization of PEGylated Liposomes. The hydrodynamic diameter, the polydispersity index (PDI), and the zeta potential of liposomes were determined by dynamic light scattering using either the Malvern Zetasizer HSA3000 or the Nanosizer ZS (both from Malvern Instruments GmbH, Herrenberg, Germany). For the size measurements, the samples were diluted with 18 MΩ-cm water to a final phospholipid concentration of 0.01 mg/mL and then recorded at 25 °C. For the zeta potential measurements, the formulations were diluted with Tris buffer (10 mM, 2 mM CsCl and pH 7.0) to a phospholipid concentration of 0.3 mg/mL.

Fluorescence Staining Experiments. The animal experiments were approved by the Ministry of Science and Research, Austria. ApoE-deficient mice with a C57Bl/6J genetic background (Charles River Laboratories, Brussels, Belgium) were fed starting at the age of 4 months with a Western-type 21% XL (raw fat) experimental food (Ssniff Spezialdiaeten GmbH, Soest, Germany) for 2−3 months. Age-matched C57Bl/6J wild-type mice (Medical University of Vienna, Austria) were used as

a control strain. The experiments were performed independent of gender because no gender-specific differences during the staining trials were observed. The endothelial layer covering the atherosclerotic lesions of ApoE-deficient mice is considered as "injured endothelium". The atherosclerotic lesions were stained with anti-CD31 to visualize the endothelial cells. For each *ex vivo* staining trial, 3–4 mice were randomly sacrificed with an overdose of isoflurane (Abbott GesmbH, Vienna, Austria). The chest was then opened, and the heart was immediately injected with PBS (pH 7.4) for 15 min to rinse the circulation. Finally, the vena cava was excised. The entire aorta, including the aortic arch (aortic specimens), was dissected, cut open, washed with PBS (pH 7.4), and transferred to an Eppendorf tube containing Krebs−Henseleit solution (118 mM NaCl; 25 mM NaHCO$_3$; 2.8 mM CaCl$_2$·2H$_2$O; 1.17 mM MgSO$_4$·7H$_2$O; 4.7 mM KCl; 1.2 mM KH$_2$PO$_4$; 2 mg/mL glucose; pH 7.4) to maintain physiological activity of the tissue. During this time, the aortic specimens were also blocked with 1% bovine serum albumin (BSA) (Sigma-Aldrich, St. Louis, MO, USA) for 1 h at room temperature to avoid unspecific binding. The samples were then incubated with the fluorescent-labeled proteins (either 10 μg/mL IL-10-Atto655 or 20 μg/mL gAd-Atto655) for 1−2 h at 37 °C and shaken in the dark to avoid fluorochrome bleaching. During the last 30 min of incubation, the samples were costained with 5 μg/mL of an anti-CD68 or anti-CD4 prelabeled antibody to visualize monocyte-derived macrophages or macrophages/T-cells, respectively. For the IL-10R *ex vivo* stainings, aortic specimens were fixed with 4% paraformaldehyde in PBS immediately after the preparation. After 30 min the specimens were blocked with 1% BSA in PBS for 30 min and then incubated with 20 μg/mL Atto488-labeled IL-10R and 5 μg/mL anti-CD31 prelabeled antibodies or 20 μg/mL of the prelabeled IgG isotype control in PBS for 1 h.

For each *in vivo* staining trial, 2−4 mice received intravenous (iv) injections into the orbital vein as followed: a total of 20 μg of IL-10-Atto655 or 4 mg of nontargeted CF-liposomes was administered to achieve the desired blood levels of 10 μg/mL IL-10-Atto655 or 2 mg/mL nontargeted CF-liposomes, respectively. These amounts were calculated assuming a total blood volume of 2 mL for an adult mouse. Notably, the applied IL-10 concentration was 10 μg/mL blood, irrespective of whether free or liposome-bound IL-10 was used. For each mouse, at 24 h postinjection, the aorta was dissected, immediately fixed with 4% paraformaldehyde in PBS for 30 min, blocked with 1% BSA in PBS for 30 min, and subsequently incubated with 5 μg/mL of an anti-CD31 or anti-CD68 prelabeled antibody. Hoechst 33342 fluorescence dye (1 μg/ mL, Invitrogen, Vienna, Austria) was added to every sample for
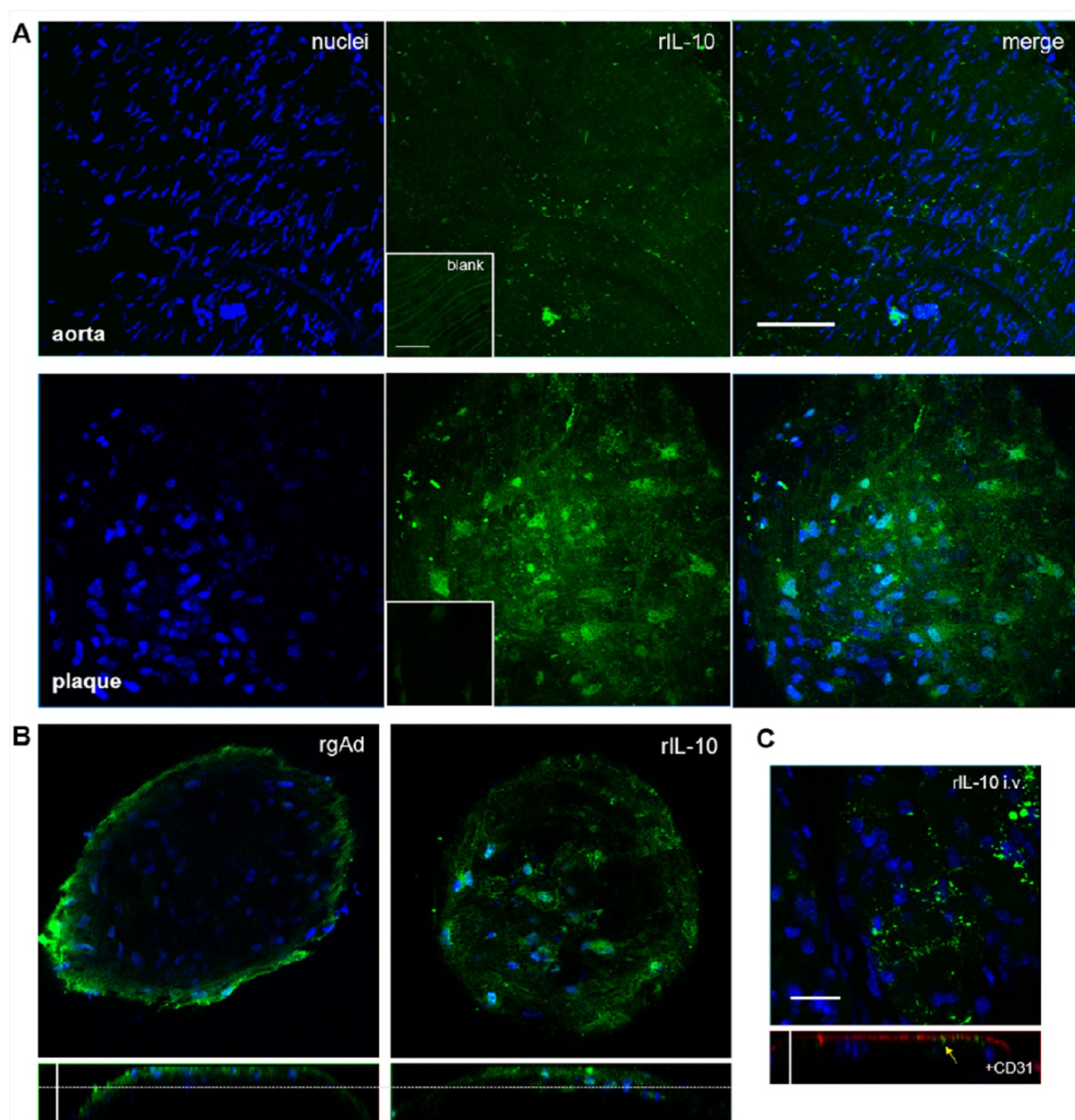
Figure 2. Recombinant IL-10 is internalized by AS plaques. Aortic specimens of ApoE-deficient and wild-type mice were incubated with Atto655 labeled IL-10 (10 μg/mL, shown in green) and stained with Hoechst nucleus dye (blue). (A) Optical sections from aortic preparations projected into one plane. For each image, a series of 20−40 fluorescence images in Z (1 μm consecutive intervals) were projected in a single image. Wild-type mouse aorta (upper panels) and AS plaques of ApoE-deficient mouse aorta (lower panels) are shown. IL-10 slightly adheres to the intact aortic endothelium, but is much more strongly internalized by AS plaques. Small insets show unstained control specimens. Both bars indicate 50 μm. (B) Single vertical and orthogonal Z-plane fluorescence images from plaques stained with recombinant gAd-Atto655 (left panels) and IL-10-Atto655 (right panels) at a depth of 15 μm (marked by the dotted lines). Vertical bar indicates 35 μm. (C) One-plane fluorescence image (upper panel) of an atherosclerotic plaque from an ApoE-deficient mouse intravenously injected with IL-10. The lower panel shows an orthogonal slide of the plaque with additional anti-CD31 endothelial-cell staining (red). The yellow arrow marks comparatively less in vivo accumulation of IL-10. Both bars indicate 20 μm.

15 min to stain the cell nuclei. Then each aortic specimen was washed 3−4 times in PBS, covered with polyvinyl alcohol mounting medium with 1,4-diazabicyclo[2.2.2]octane (Sigma-Aldrich), adjusted under a stereomicroscope with the intra-vascular side on the glass slide surface, and pressed with a coverslip. A picture showing the orientation of the specimens is outlined in the Supporting Information, Figure S3A.

Fluorescence Imaging. All fluorescence and transmitted light images (Z-stack scans) of the aortic samples and cultured cells were acquired using the LSM 510 META Axiovert 200 M Zeiss confocal system (Jena, Germany), operating with a 25 mW laser diode tuned to 405 nm for Hoechst staining of the cell nuclei, a 30 mW argon laser tuned to 488 nm for visualization of the AF488-labeled antibodies, and a 5 mW HeNe laser tuned to 633 nm for visualization of all Atto655-labeled proteins. Images were collected using a 40× Plan-Neofluar 1.3 DIC oil immersion objective and a multitrack configuration, whereby the Hoechst, AF488, and Atto655
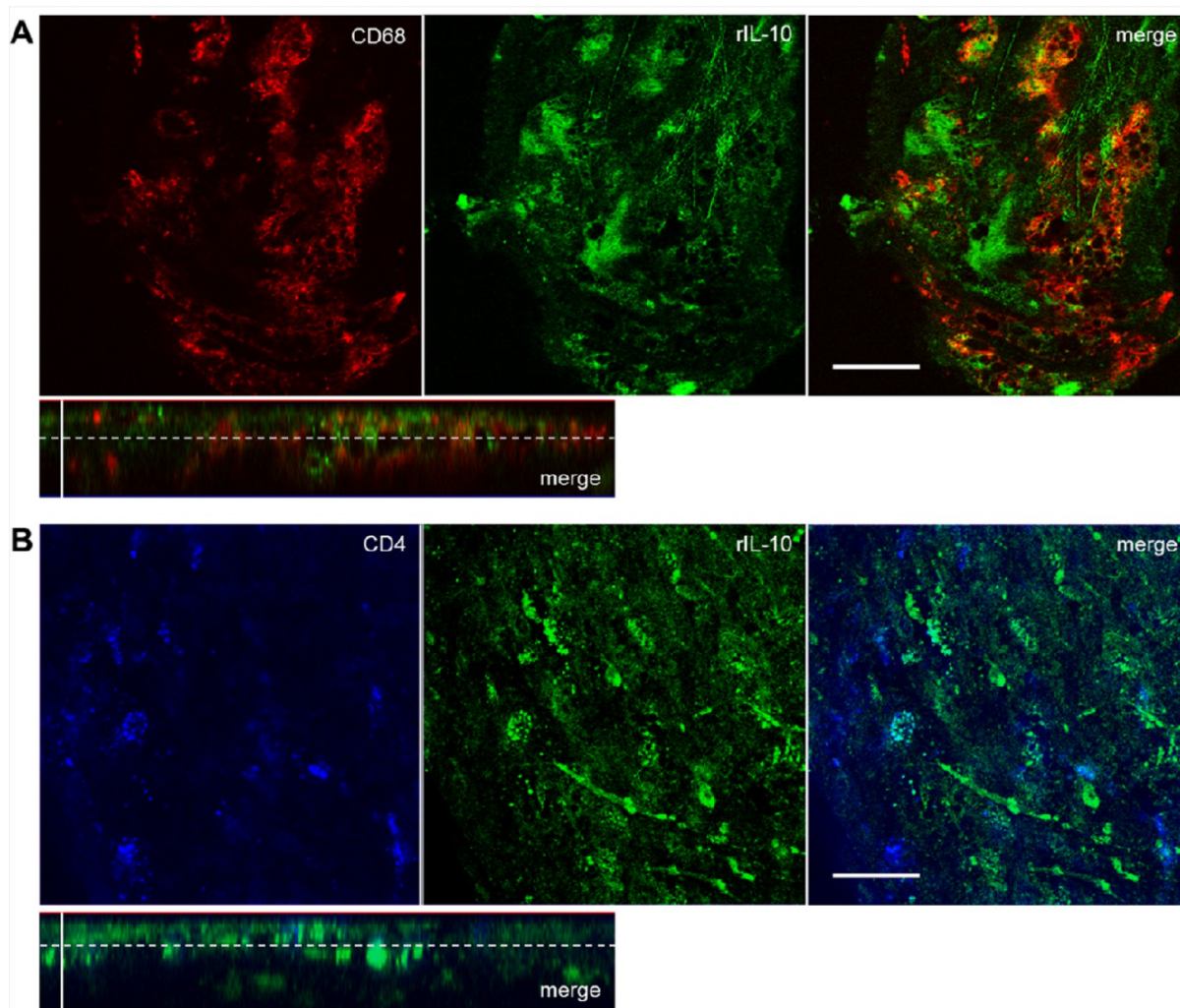
Figure 3. Recombinant IL-10 is localized predominantly in the foam cell area of atherosclerotic plaques. For double-staining experiments, aortic specimens of ApoE-deficient mice were coincubated with IL-10-Atto655 (10 μg/mL, shown in green) and AlexaFluor ready-labeled rat anti-mouse antibodies (5 μg/mL). Single Z-plane fluorescence images of AS plaques were taken at a depth of 8 μm (marked by the dotted lines in the orthogonal sections). (A) Double staining of IL-10 (green) with an anti-CD68 monocyte/macrophage marker (shown in red). Partial colocalization is seen in the merged images. Horizontal bar indicates 25 μm; vertical bar indicates 20 μm. (B) Double staining of IL-10 with an anti-CD4 T-cell/macrophage marker (blue). Partial colocalization is seen in the merged images. Horizontal bar indicates 25 μm.

signals were sequentially collected with BP 420−480 nm, BP 505−550 nm, and BP 679−743 nm filters after excitation with 405 nm, 488 nm, and 633 nm laser lines, respectively. The Zeiss AIM software version 4.2 was used for all of the data collection. All confocal images were acquired with a frame size of 512 × 512 or 1024 × 1024 pixels averaged three times. Adobe Photo Shop CS5 was used for the end-processing of all acquired images. A picture showing the orientation of the images is outlined in the Supporting Information, Figure S3B.

Immunization Experiments. Female Balb/c mice (Charles River Laboratories, Sulzfeld, Germany), aged 8 weeks, were treated according to European Community rules of animal care with the permission of the Austrian Ministry of Science (BMWF-66.009/0172-II/3b/2011). Mice (n = 8/group) were intravenously injected with (1) PEGylated liposomes that are coated with recombinant IL-10 [IL-10-liposomes; 100 μL/application, lipid concentration = 10 mg/mL (i.e., 1 mg of lipid/mouse), concentration of IL-10 = 70 μg/mL (i.e., 7 μg of IL-10/mouse)], (2) PEGylated liposomes [lipid concentration = 10 mg/mL (i.e., 1 mg of lipid/mouse)],

or (3) recombinant IL-10 [70 μg/mL (i.e., 7 μg of IL-10/mouse)], or (4) remained untreated. Immunizations were performed on days 7, 21, 35, and 49, and blood was drawn on days 0, 14, 28, 42, 56, and 70.

Intradermal skin tests and evaluation of cytokines in stimulated spleen cells were performed as described in the Supporting Information.

Detection of Total Serum Immunoglobulins by ELISA. Antibody detection of total amounts of IgG, IgM, IgA, or IgE was performed by ELISA as described previously[32] with modifications. Briefly, the microtiter plates (Maxisorp, Nunc, Roskilde, Denmark) were coated with rat anti-mouse antibodies for IgE, IgM, or IgA (BD Pharmingen, Schwechat, Austria; all 200 ng/mL in Na-bicarbonate puffer, pH 8.3) or rat anti-mouse IgG (Bethyl Laboratories, USA; 2,000 ng/mL). A standard curve was created from the dilution of mouse isotype standards IgG, IgM, IgA, and IgE (BD Pharmingen, Schwechat, Austria). The starting concentration was 25 ng/mL for IgE and 100 ng/mL for IgM, IgA, and IgG. Further dilution steps were in a 1:2 ratio. Mouse sera were diluted 1:20 for IgE, 1:5000 for IgM and
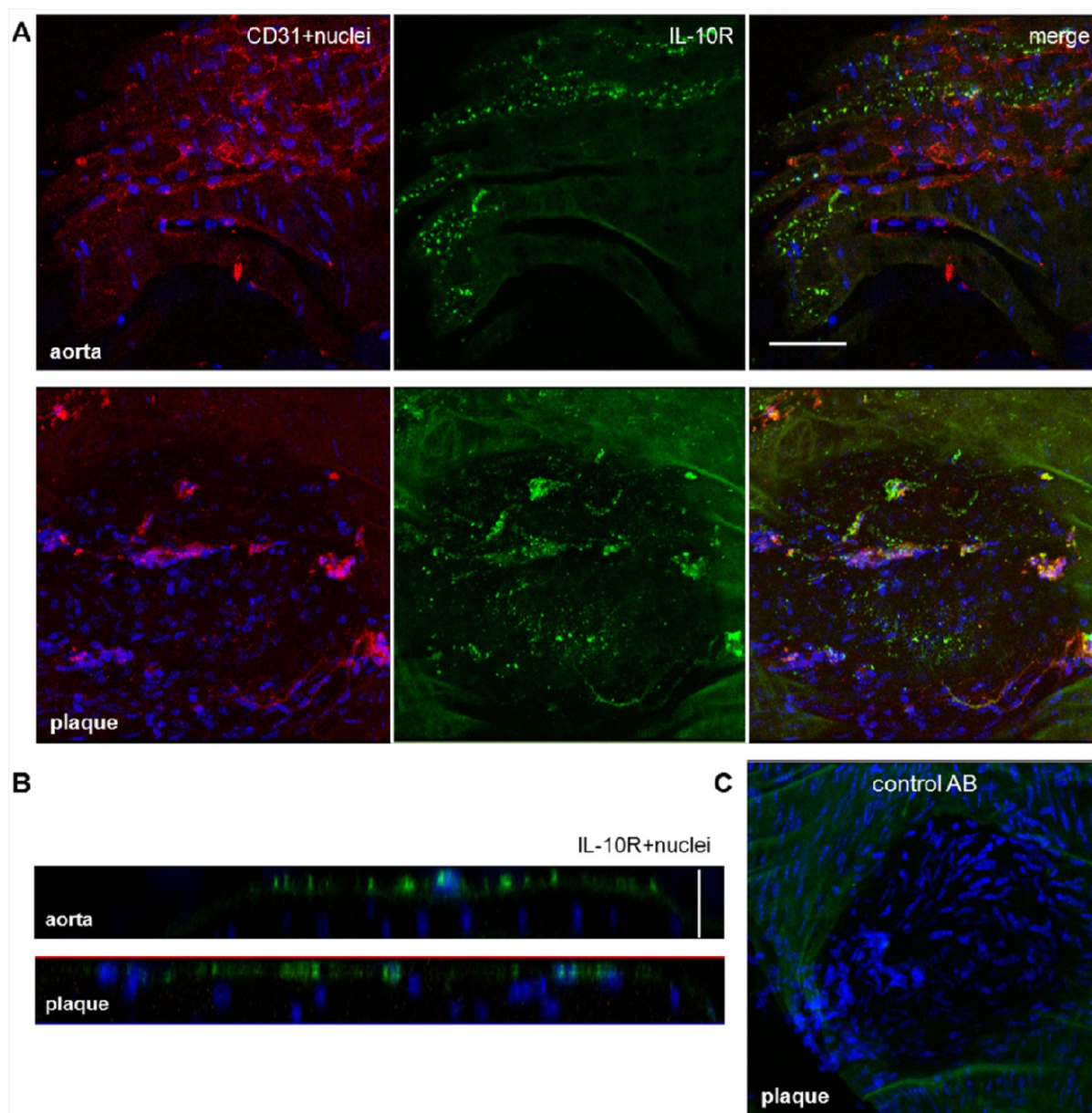
Figure 4. IL-10 receptor is localized on the surface of the aortic endothelium from ApoE-deficient mice. (A) One-plane images of aortic specimens from ApoE- deficient mice coincubated with AF488 labeled anti-IL-10R antibody (20 μg/mL, green) and AF635 ready-labeled anti-CD31 antibody (5 μg/mL, red). IL-10R was detected on uninjured specimens and on atherosclerotic plaques; no direct colocalization between IL-10R and CD31 was found. Bar indicates 50 μm. (B) Single orthogonal Z-plane fluorescence images from the aortic endothelium of ApoE-deficient mice showing the localization of IL-10R on the endothelial surface. Vertical bar indicates 25 μm. (C) One-plane image of an aortic section with AS plaque showing the negative staining with an AF488 ready labeled isotype control antibody. All specimens were stained with Hoechst nucleus dye (blue).

IgA, and 1:10000 for IgG detection. Peroxidase-labeled anti-mouse antibodies (Bethyl Laboratories, USA) were used in a 1:10,000 ratio. Detection was performed with TMB solution (BD Bioscience, Vienna, Austria) and measured at 450−630 nm.

Detection of Serum Antiliposome-Antibodies by ELISA. Detection of IgM- or IgG-antibodies directed against liposomes was performed by ELISA as described above, with slight modifications: the microtiter plates were coated with PEGylated liposomes (lipid concentration = 5 mg/mL in 50 μL/well). Isotype standard antibodies (BD Pharmingen, Schwechat, Austria) were used for dilution series to create standard curves (the starting concentration was 50 ng/mL for IgM and IgG; further dilution steps were in a 1:2 ratio). Sera

were diluted 1:2000 for IgM and 1:4000 for IgG. Peroxidase-labeled anti-mouse IgM or IgG antibodies (Bethyl Laboratories, USA) were used in a 1:10000 ratio. Detection was performed with TMB solution (BD Bioscience, Vienna, Austria) and measured at 450−630 nm.

Statistical Analysis. Differences between the groups for values of IgM antibodies in immune sera were analyzed by one-way ANOVA with a Newman−Keuls post hoc test. For comparison of IgM antibodies before and after immunizations within one group, a t-test was applied. Data analysis was performed using Prism V software (GraphPad, La Jolla, CA, USA). A value of $p < 0.05$ was considered statistically significant.
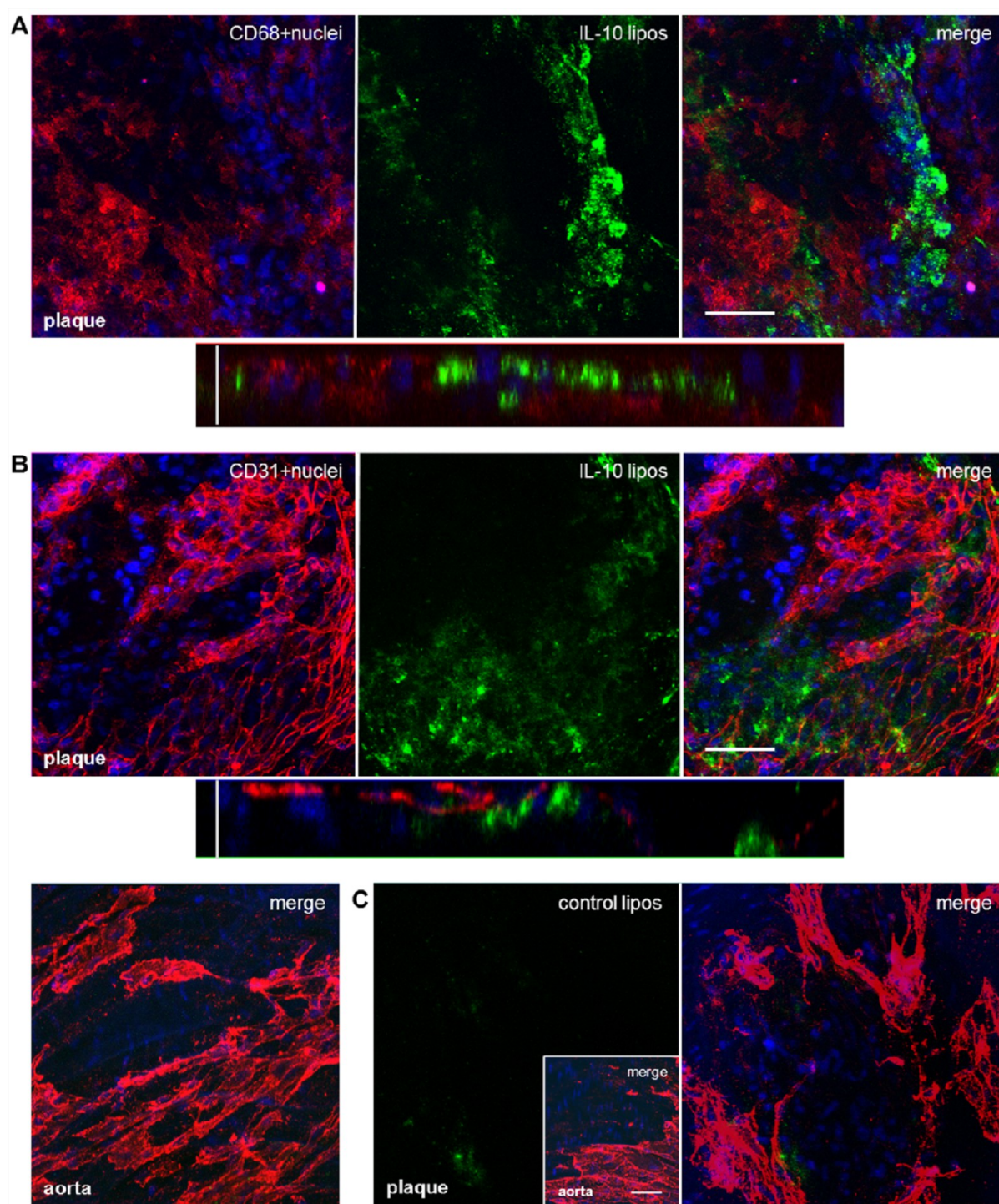
Figure 5. IL-10-targeted PEGylated liposomes are internalized by atherosclerotic plaques after in vivo injection. ApoE-deficient mice were injected with CF-labeled IL-10-targeted stealth liposomes (green). After 24 h, aortic specimens were dissected, costained with AF635 ready-labeled rat anti-mouse antibodies (5 μg/mL, red) and Hoechst nucleus dye (blue), and imaged by CLSM. (A) One-plane and single orthogonal Z-plane fluorescence images from an AS plaque costained with an anti-CD68 monocyte/macrophage marker. Horizontal bar indicates 50 μm, vertical bar 25 μm. (B) The same as shown in panel A, but costained with an anti-CD31 endothelial-cell marker (upper and middle panels). The IL-10-CF-liposomes did not accumulate at the uninjured aortic endothelium (lower panel). (C) Aortic specimens of ApoE-deficient mice dissected 24 h after injection of CF-labeled untargeted liposomes. The CF-liposomes did not accumulate at the uninjured aortic endothelium (small inset) and were just slightly internalized by AS plaques. Bar in inset indicates 50 μm.

■ RESULTS

Characterization of IL-10-Targeted PEGylated Liposomes. IL-10 was covalently coupled to the distal end of functionalized PEG-lipids incorporated in preformed lip-

osomes. The final protein concentration was 50.7 μg of IL-10/mL at a lipid concentration of 10 mg/mL, corresponding to a calculated average of 92 IL-10 molecules per liposome (the calculations are given in the Supporting Information). The

average hydrodynamic diameter of untargeted liposomes was 183.9 ± 0.8 nm with PDI values of 0.06 ± 0.02. The size remained essentially the same (184.5 ± 1.6 nm and PDI values of 0.09 ± 0.01, $n = 3$) upon coupling IL-10, while the zeta potential values decreased from -10.2 ± 0.2 mV to -18.6 ± 0.2 mV.

Recombinant IL-10 Is Internalized by Atherosclerotic Plaques. To evaluate the affinity of IL-10 to AS lesions, aortic specimens of ApoE-deficient and wild-type mice were stained with IL-10-Atto655 and visualized by CLSM. Even though AS lesions were not detected in the aortic specimens of wild-type mice, a slight fluorescent signal of IL-10-Atto655 was present on the surface of the aortic endothelium (Figure 2A, upper panels). ApoE-deficient mice had an abundance of AS plaques. The less injured area between the plaques showed the same weak accumulation of IL-10 as in the control mice. However, the IL-10 signal detected at the AS lesions was much stronger and was found to be internalized in single cells inside the plaque (Figure 2A, lower panels).

To assess the targeting behavior of IL-10 to AS plaques, we compared the staining patterns of IL-10-Atto655 to those obtained for Atto655-labeled recombinant globular adiponectin (gAd-Atto655). gAd-Atto655 was recently identified by our group as a promising targeting protein for AS plaques,[30] and it is well suited for direct comparison because of its similar molecular weight to IL-10 (gAd 17 kDa versus IL-10 19 kDa). We stained AS plaques, as described above, using gAd and IL-10 applied in equal concentrations corresponding to the labeled fluorescent dye. As seen in Figure 2B, we observed remarkable differences in the staining pattern. While gAd accumulated in the outer AS plaque areas (left panels), IL-10 preferentially penetrated the plaques (right panels). These different staining characteristics clearly point to a protein-specific uptake of IL-10 into AS plaques, irrespective of the fluorescent dye.

Recombinant IL-10 Is Localized Predominantly in the Foam Cell Area of Atherosclerotic Plaques. To characterize the localization of IL-10 in AS plaques, we performed *ex vivo* costaining experiments. Due to the observation that the IL-10 internalizing cells in the plaques showed a morphology typical of foam cells, an anti-CD68 monocyte/macrophage marker and an anti-CD4 T-cell/macrophage marker were used for costaining. Monocyte-derived macrophages and T-helper cells[33] are the main cells to enter the AS plaque scenario. Double staining confirmed a partial colocalization of IL-10-Atto655 with both markers, CD68 (Figure 3A) and CD4 (Figure 3B), which is apparent in the merged images of Figure 3. This observation and the consistent macrophage-like morphology of the IL-10 internalizing cells suggest that the "IL-10 internalizing cells" are predominantly macrophages.

IL-10 Receptor Is Localized on the Surface of the Aortic Endothelium from ApoE-Deficient Mice. To examine whether the expression of IL-10 receptors at the aortic endothelium differs between uninjured and AS tissues, we stained aortic specimens of ApoE-deficient mice with a fluorescent-labeled antibody against the only known receptor for IL-10 (IL-10 receptor complex). A strong fluorescence pattern was detected on the surface of the uninjured aortic endothelium (Figure 4A). The pattern was even stronger at the surface of AS plaques (Figure 4B). As a negative control, aortic specimens of ApoE-deficient mice were stained with a rat-IgG isotype control. We did not detect any binding of unspecific IgG at the uninjured aortic endothelium or on AS plaques (Figure 4C).

IL-10R was found mainly on the surface of both uninjured and AS plaque aortic tissue. IL-10-Atto655 was also found on the surface of uninjured aortic tissue. In contrast, in cases of AS plaque, it was largely internalized into the plaque stroma.

The observed lack of penetration of the IL-10R antibody into deeper sections of the aortic specimen may be due to limitations in the staining method. For instance, the IL-10R antibody had a markedly higher molecular weight in comparison to the recombinant IL-10 molecule. Furthermore, the fact that the samples consisted of the entire aorta, instead of histologically prepared sections, may also have decreased the staining efficiency. However, we preferred using the entire aorta to maintain more physiologically accurate conditions.

***In Vivo* Targeting of AS Plaques with Recombinant IL-10.** To test the targeting potential of IL-10 under *in vivo* conditions, IL-10-Atto655 was injected into ApoE-deficient mice at the same concentration as was used in the *ex vivo* experiments (i.e., the blood concentration of IL-10-Atto655 after injection was the same as used during the *ex vivo* incubation). At 24 h after injection, the aortic specimens were dissected and visualized *ex vivo*. The CLSM images showed only a very weak, spotty IL-10 signal on the surface of AS plaques. The surface was made apparent by CD31 endothelial staining (Figure 2C). This indicates an unspecific adherence of IL-10-Atto655 on the surface of AS plaques when applied *in vivo*.

IL-10-Targeted PEGylated Liposomes Are Internalized by Atherosclerotic Plaques after an Intravenous Injection. To achieve an improved stability in the circulation, recombinant unlabeled IL-10 was coupled with PEGylated liposomes. For *in vivo* trials, we used the same amount of IL-10 as before, but the liposomes can adhere more signal emitting molecules than free IL-10. ApoE-deficient mice were sacrificed 24 h postinjection. Afterward, through CLSM imaging, we observed an accumulation of IL-10-targeted liposomes within the AS plaques. This was similar to the staining pattern found when IL-10-Atto655 was used during the *ex vivo* incubation experiments. *Ex vivo* staining of aortic sections with anti-CD68 showed a localization of the IL-10-CF-liposomes around the macrophage-rich areas within AS plaques (Figure 5A). Staining with anti-CD31 did not show any colocalization of IL-10-CF-liposomes with endothelial cells (Figure 5B). Also, IL-10-CF-liposomes did not accumulate at the uninjured aortic endothelium. Untargeted CF-liposomes, used as a negative control, were unspecific, only slightly internalized by AS plaques (Figure 5C).

Evaluation of Total and Antiliposome-Antibodies in Sera of Balb/c Mice. When evaluating the total antibody levels of IgA, IgM, IgG, and IgE in mouse sera, none of the tested antibody classes were affected during iv treatments with IL-10-liposomes, nontargeted liposomes, or IL-10 (data not shown). Investigation of IgM and IgG against liposomes revealed a significant increase of IgM-antibody levels from the preimmune serum samples to the final immune serum samples in the groups intravenously treated with IL-10-liposomes or liposomes (Figure 6). However, the increase was significantly lower in the group injected with IL-10-liposomes than in the liposome group that was not coated with IL-10. No increase in IgG-antibodies against liposomes was observed in any of the groups (data not shown).

Intradermal Skin Tests. To rule out any specific sensitization by iv treatments with the particles, mice were subjected to intradermal skin testing. Immediate type I skin
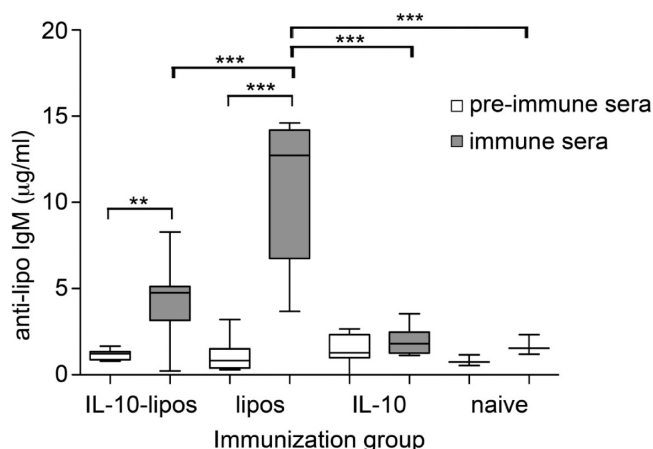
Figure 6. Evaluation of antiliposome-antibodies in sera. After immunization of Balb/c mice, IgM- or IgG-antibodies directed against liposomes were detected by ELISA. A significant increase of IgM-antibodies directed against liposomes was induced by immunizations with IL-10-liposomes iv and nontargeted liposomes iv. Importantly, the targeting of liposomes with IL-10 significantly reduced the increase of IgM-antibodies ($**p < 0.01$, $***p < 0.001$). Boxes represent the range of the inner quartiles of the samples divided by the median, and whiskers represent the smallest and the highest value, respectively, of duplicates from two independent experiments.

reactivity was seen after intradermal testing with (1) IL-10 alone in 3/8 of the animal group immunized with IL-10-liposomes and with (2) IL-10-liposomes in 2/8 of the entire mouse groups, including naive mice (data not shown). All other test substances (nontargeted liposomes, codfish, PBS) did not provoke positive type I skin test reactions, except for the positive control (histamine releasing compound 48/80).

Evaluation of Cytokines in Stimulated Spleen Cells. Isolated splenocytes of mice were stimulated with medium (control), liposomes, IL-10-liposomes, or concanavalin A. The released cytokines were analyzed via multiplex analysis in FACS.[34] IL-2 levels were elevated, in comparison to the control group, in all groups after either IL-10-liposome stimulation (50.65 to 61.45 pg/mL) or liposomes alone (47.08 to 84.60 pg/mL). After stimulation with liposomes, TNF-α levels were the lowest in the group of mice immunized with IL-10. Stimulation with IL-10-liposomes increased TNF-α release in splenocytes of mice immunized with IL-10-liposomes (Figure S4 in the Supporting Information). None of the other examined cytokines (IL-1α, IL-2, IL-4, IL-5, IL-6, IL-10, IL-17, IFN-γ, GM-CSF) showed levels that were elevated above the control.

■ DISCUSSION

Atherosclerosis is a chronic disease in which inflammatory processes are one of the main driving forces, leading to the formation, progression, and rupture of AS plaques.[35] The identification of, and the ability to follow, the development of AS lesions are still major challenges for medical imaging which is limited not only by the performance of present imaging techniques but also by the availability of specific molecules for targeting.[36] Consequently, several mediators involved in the inflammatory scenario during the progression of AS have been suggested and tested to recognize AS lesions.[37,38] Many of these studies focus on proinflammatory mediators, but little on anti-inflammatory mediators.[36]

Recently, a study by Pinderski Oslund et al. found that activated T-lymphocytes overexpress the anti-inflammatory cytokine IL-10, and that this event is capable of blocking AS actions *in vitro* and *in vivo*.[39,40] Furthermore, IL-10 expression is elevated in advanced and unstable AS plaques. This fact suggests that IL-10 contributes to the regulation of the local inflammatory response and works against excessive cell death in the plaques.[41−43] Thus, it was suggested that IL-10 may arrest and reverse the chronic inflammatory response in established AS.[44]

Due to the prevalence and the predicted anti-inflammatory actions of IL-10 in AS plaques, we considered IL-10 as a promising protein, not only for AS regression studies but also for the detection of specific areas in the AS scenario. Hence, this study was designed to evaluate whether recombinant IL-10 is applicable to AS imaging. First, we used fluorescent-labeled IL-10 for *ex vivo* staining. By incubating aortic specimens from ApoE-deficient mice with IL-10, we found that IL-10 becomes efficiently internalized by AS plaques and only slightly adheres to the surrounding aortic endothelium. To examine the targeting potential of IL-10 in more detail, we compared the staining patterns of IL-10-Atto655 with gAd-Atto655, a recently identified promising marker for AS.[30] While gAd-Atto655 was detected in the fibrous cap of the plaques, IL-10-Atto655 accumulated inside the plaque stroma, largely in macrophages positive for CD68 and CD4. The purpose of the comparative analysis of the two potential protein targeting structures was to outline the possibility of imaging distinct areas in AS plaques and to distinguish between the different stages of plaque formation.

To better understand whether the IL-10 receptor complex is involved in the uptake of recombinant IL-10 by AS plaques, aortic specimens from ApoE-deficient mice were stained with an anti-IL-10R antibody. We found that IL-10R is expressed on the surface of the aortic endothelium, corresponding to the staining pattern of IL-10-Atto655. Moreover, IL-10R was expressed more strongly at AS plaques than at the uninjured endothelium. However, the expression was preferentially on the surface and not inside the plaques, where we found IL-10-Atto655 largely accumulated inside macrophages. Crawly et al. have shown that IL-10 can mediate its anti-inflammatory effects independently of IL-10R. They also suggested that multiple and distinct signaling pathways mediate the various pleiotropic activities of IL-10.[45] Therefore, the high expression levels of IL-10R might be involved in the binding and uptake of IL-10-Atto655 to AS plaques; whereas, the internalization into plaque macrophages might follow an IL-10 receptor complex-independent uptake mechanism.

Next, we tested the *in vivo* performance of IL-10-Atto655 in the ApoE-deficient mouse model. In these experiments, only a slight accumulation on the surface of the plaques was observed. It is known that IL-10 is a rather unstable protein, normally forming homodimers which bind to corresponding receptors.[46,47] Recombinant and predominantly monomeric IL-10 may not be stable enough to enter the AS scenario after iv injection because of its short *in vivo* half-life and the potentially destabilizing fluorescence labeling process. Thus, we speculate that the low *in vivo* stability of IL-10 would critically limit its usability as a target molecule in clinical AS plaque detection.

One way to circumvent this shortcoming is to couple the protein to slowly degrading nanoparticles. Nanoparticle research is an emerging field that is expanding into optical and biomedical fields.[48] Liposomes are one of the most widely

studied classes of nanoparticles primarily because various labels can easily be linked to, or incorporated within, the liposomal bilayer.[49,50]

To utilize this approach, we coupled recombinant unlabeled IL-10 to carboxyfluorescein-labeled stealth liposomes in order to prolong the half-life of IL-10 in the circulation and, thus, be able to recognize AS plaques. In addition to prolonging the IL-10 circulation time, a single nanoparticle can transport a higher payload of fluorescent dyes or contrast agents (e.g., gadolinium, iron particles) for nuclear magnetic resonance imaging (NMRI), which is of potential interest for future clinical applications. By themselves, sensitive protein structures, such as IL-10, cannot be loaded with too many signal emitting molecules without risking the protein's loss of target specificity. We found that 24 h postinjection, IL-10-targeted CF-liposomes accumulated inside the AS plaques. Fluorescently labeled IL-10 detected AS plaques in *ex vivo* experiments, but showed less usability in *in vivo* experiments. The fact that the nanoconstruct was able to enter the AS plaque implies that the liposomes successfully stabilized IL-10 in the circulation. There was no detected adherence of the nanoconstruct to the uninjured aortic endothelium, suggesting that the overall capacity of IL-10 was modified by the liposomes to be more specific to AS plaques. Nontargeted CF-liposomes did not show any binding affinity to the uninjured endothelium, and were only slightly internalized by AS plaques. These observations point to a plaque-specific accumulation of IL-10-targeted liposomes and are in agreement with the function of the PEG layer to protect liposomes from effective immunological recognition *in vivo*.

In general, PEGylated stealth liposomes are reported to remain in the circulation for up to 48 h, increasing the opportunity for an efficient target−ligand interaction.[49,50] However, according to our previous experiments, the majority of untargeted liposomes end up in the liver, kidneys, and spleen within the first few hours postinjection.[51] Nonetheless, our nanocargo system is advantageous because multiple targeting structures can be properly bound to the surface of each liposome: in our case, approximately 90 protein molecules are covalently linked to the liposome particle. This feature may significantly enhance the targeting efficiency of liposomes, even when the time the particles are circulating in the system is less than 24 h. In this context, it will be of importance to clarify the uptake time of IL-10 targeted liposomes in critically activated areas of the AS plaques. In the future, this may be realized by magnetic resonance imaging in combination with targeted nanocargos (i.e., iron oxide loaded liposomes).[52]

Due to Lauw et al.'s finding that an overproduction of inflammatory cytokines in humans was caused by recombinant human IL-10 in a dose dependent manner,[53] we suspected that the immunogenic properties of IL-10 coated liposomes could be a major limitation in their clinical use. To investigate this limitation, we examined the immunological properties of IL-10-coated liposomes. Different particle preparations were applied to BALB/c mice intravenously four times with an interval of 14 days. We did not observe an increase in the total antibody levels of IgM, IgA, IgE, or IgG in the sera of these mice. However, an increase in IgM-antibodies specifically directed against liposomes was seen in the groups immunized with IL-10-liposomes or nontargeted liposomes. In accordance with a previous study, we assume that the IgM-antibodies are directed against polyethylene glycol (PEG).[54] Furthermore, we found that the IgM-antibody increase was significantly lower in the group injected with IL-10-liposomes as compared to non-

targeted liposomes. This result points toward the anti-inflammatory properties of IL-10.

Still, in intradermal skin tests, a moderate type I skin reaction to IL-10 was found in 3 out of 8 mice immunized with IL-10-liposomes. We hypothesize from this result that IL-10-targeted liposomes could induce antibody-mediated hypersensitvitiy to IL-10 in some cases. This is in contrast to a previously reported mouse model of asthma, where subcutaneous application of an IL-10-vaccine induced IgG-antibodies against self-IL-10, which unexpectedly enhanced the desirable bioactivity of IL-10 *in vivo* and *in vitro*, thereby ameliorating airway inflammation.[55]

To examine the potential immune responses toward nontargeted or IL-10-functionalized liposomes on the T-cell level, cytokine release from cultured splenocytes upon stimulation was examined. Among the tested cytokines, only TNF-α levels were enhanced above medium control. Highest TNF-α levels were released when splenocytes were stimulated with nontargeted liposomes, also in naive animals. This response indicated that a TNF-α response to liposomes was most probably an *in vitro* effect. The release could be suppressed when stimulation with IL-10-liposomes was performed in splenocytes of naive mice, or animals immunized with soluble IL-10 or nontargeted liposomes. This might be attributable to the known anti-inflammatory properties of recombinant IL-10 *in vitro*, which could reduce the release of the proinflammatory cytokine TNF-α.[56]

However, when mice were immunized with IL-10-coupled liposomes, IL-10 could not sufficiently counteract the TNF-α release. This indicates that a specific immune response comprising antibody formation and T-cell reactivity was induced by the repeated injections of IL-10-coupled liposomes during our stringent immunization protocol, including several applications in short time intervals. Therefore, to prevent specific sensitization toward IL-10 during *in vivo* imaging, applications should possibly be restricted to once or twice in a lifetime and performed with longer time intervals in between.

Taken together, we showed that recombinant IL-10 preferentially accumulates in AS plaque areas. Nanoconstructs of IL-10 and PEGylated liposomes increase IL-10s stability *in vivo* and the specificity of target recognition, similar to globular adiponectin nanoconstructs.[57] Thus, IL-10 combined with multifunctionalized liposomes is a promising candidate for multimodal AS plaque imaging.

■ ASSOCIATED CONTENT

ⓈSupporting Information

Fluorescent-labeling procedure of IL-10, molecular calculations, liposome preparation and the experimental details for the intradermal skin tests as well as the evaluation of cytokines in stimulated spleen cells; Figure S1 depicting the Atto655 fluorescence labeling of recombinant mouse IL-10, verified by SDS−PAGE and Western blot techniques; Figure S2 showing the preparation of PEGylated stealth liposomes; Figure S3 depicting the orientation of the aortic specimens for CLSM imaging; Figure S4 showing cytokine levels for TNF-α in supernatants of stimulated splenocytes obtained from Balb/c mice. This material is available free of charge via the Internet at http://pubs.acs.org.

■ AUTHOR INFORMATION

Corresponding Author
*Head of the Research Unit on Lifestyle and Inflammation-Associated Risk Biomarkers, Clinical Institute of Medical and

Chemical Laboratory Diagnostics, Auenbruggerplatz 15, 8036 Graz, Austria. Tel: +43 316 385 83340. Fax: +43 316 385 4024. E-mail: harald.mangge@klinikum-graz.at.

Author Contributions

§These authors contributed equally to this study.

Notes

The authors declare no competing financial interest.

■ **REFERENCES**

(1) Rocha, V. Z.; Libby, P. Obesity, inflammation, and athero-sclerosis. *Nat. Rev. Cardiol.* **2009**, *6* (6), 399−409.

(2) Sanz, J.; Fayad, Z. A. Imaging of atherosclerotic cardiovascular disease. *Nature* **2008**, *451* (7181), 953−7.

(3) Helft, G.; Worthley, S. G.; Fuster, V.; Fayad, Z. A.; Zaman, A. G.; Corti, R.; Fallon, J. T.; Badimon, J. J. Progression and regression of atherosclerotic lesions: monitoring with serial noninvasive magnetic resonance imaging. *Circulation* **2002**, *105* (8), 993−8.

(4) Camici, P. G.; Rimoldi, O. E.; Gaemperli, O.; Libby, P. Non-invasive anatomic and functional imaging of vascular inflammation and unstable plaque. *Eur. Heart J.* **2012**, *33* (11), 1309−17.

(5) Packard, R. R.; Libby, P. Inflammation in atherosclerosis: from vascular biology to biomarker discovery and risk prediction. *Clin. Chem.* **2008**, *54* (1), 24−38.

(6) Fiorentino, D. F.; Bond, M. W.; Mosmann, T. R. Two types of mouse T helper cell. IV. Th2 clones secrete a factor that inhibits cytokine production by Th1 clones. *J. Exp. Med.* **1989**, *170* (6), 2081−95.

(7) Moore, K. W.; Vieira, P.; Fiorentino, D. F.; Trounstine, M. L.; Khan, T. A.; Mosmann, T. R. Homology of cytokine synthesis inhibitory factor (IL-10) to the Epstein-Barr virus gene BCRFI. *Science* **1990**, *248* (4960), 1230−4.

(8) Commins, S.; Steinke, J. W.; Borish, L. The extended IL-10 superfamily: IL-10, IL-19, IL-20, IL-22, IL-24, IL-26, IL-28, and IL-29. *J. Allergy Clin. Immunol.* **2008**, *121* (5), 1108−11.

(9) de Waal Malefyt, R.; Abrams, J.; Bennett, B.; Figdor, C. G.; de Vries, J. E. Interleukin 10(IL-10) inhibits cytokine synthesis by human monocytes: an autoregulatory role of IL-10 produced by monocytes. *J. Exp. Med.* **1991**, *174* (5), 1209−20.

(10) Peguet-Navarro, J.; Moulon, C.; Caux, C.; Dalbiez-Gauthier, C.; Banchereau, J.; Schmitt, D. Interleukin-10 inhibits the primary allogeneic T cell response to human epidermal Langerhans cells. *Eur. J. Immunol.* **1994**, *24* (4), 884−91.

(11) Fiorentino, D. F.; Zlotnik, A.; Mosmann, T. R.; Howard, M.; O'Garra, A. IL-10 inhibits cytokine production by activated macro-phages. *J. Immunol.* **1991**, *147* (11), 3815−22.

(12) O'Garra, A.; Vieira, P. T(H)1 cells control themselves by producing interleukin-10. *Nat. Rev. Immunol.* **2007**, *7* (6), 425−8.

(13) Le Gros, G.; Erard, F. Non-cytotoxic, IL-4, IL-5, IL-10 producing CD8+ T cells: their activation and effector functions. *Curr. Opin. Immunol.* **1994**, *6* (3), 453−7.

(14) Fillatreau, S.; Gray, D.; Anderton, S. M. Not always the bad guys: B cells as regulators of autoimmune pathology. *Nat. Rev. Immunol.* **2008**, *8* (5), 391−7.

(15) Ryan, J. J.; Kashyap, M.; Bailey, D.; Kennedy, S.; Speiran, K.; Brenzovich, J.; Barnstein, B.; Oskeritzian, C.; Gomez, G. Mast cell

homeostasis: a fundamental aspect of allergic disease. *Crit. Rev. Immunol.* **2007**, *27* (1), 15−32.

(16) Moore, K. W.; de Waal Malefyt, R.; Coffman, R. L.; O'Garra, A. Interleukin-10 and the interleukin-10 receptor. *Annu. Rev. Immunol.* **2001**, *19*, 683−765.

(17) Williams, L. M.; Ricchetti, G.; Sarma, U.; Smallie, T.; Foxwell, B. M. Interleukin-10 suppression of myeloid cell activation–a continuing puzzle. *Immunology* **2004**, *113* (3), 281−92.

(18) Chernoff, A. E.; Granowitz, E. V.; Shapiro, L.; Vannier, E.; Lonnemann, G.; Angel, J. B.; Kennedy, J. S.; Rabson, A. R.; Wolff, S. M.; Dinarello, C. A. A randomized, controlled trial of IL-10 in humans. Inhibition of inflammatory cytokine production and immune responses. *J. Immunol.* **1995**, *154* (10), 5492−9.

(19) Goudy, K.; Song, S.; Wasserfall, C.; Zhang, Y. C.; Kapturczak, M.; Muir, A.; Powers, M.; Scott-Jorgensen, M.; Campbell-Thompson, M.; Crawford, J. M.; Ellis, T. M.; Flotte, T. R.; Atkinson, M. A. Adeno-associated virus vector-mediated IL-10 gene delivery prevents type 1 diabetes in NOD mice. *Proc. Natl. Acad. Sci. U.S.A.* **2001**, *98* (24), 13913−8.

(20) Donnelly, R. P.; Dickensheets, H.; Finbloom, D. S. The interleukin-10 signal transduction pathway and regulation of gene expression in mononuclear phagocytes. *J. Interferon Cytokine Res.* **1999**, *19* (6), 563−73.

(21) Carson, W. E.; Lindemann, M. J.; Baiocchi, R.; Linett, M.; Tan, J. C.; Chou, C. C.; Narula, S.; Caligiuri, M. A. The functional characterization of interleukin-10 receptor expression on human natural killer cells. *Blood* **1995**, *85* (12), 3577−85.

(22) Jurlander, J.; Lai, C. F.; Tan, J.; Chou, C. C.; Geisler, C. H.; Schriber, J.; Blumenson, L. E.; Narula, S. K.; Baumann, H.; Caligiuri, M. A. Characterization of interleukin-10 receptor expression on B-cell chronic lymphocytic leukemia cells. *Blood* **1997**, *89* (11), 4146−52.

(23) Mosser, D. M.; Zhang, X. Interleukin-10: new perspectives on an old cytokine. *Immunol. Rev.* **2008**, *226*, 205−18.

(24) Wickline, S. A.; Neubauer, A. M.; Winter, P. M.; Caruthers, S. D.; Lanza, G. M. Molecular imaging and therapy of atherosclerosis with targeted nanoparticles. *J. Magn. Reson. Imaging* **2007**, *25* (4), 667−80.

(25) Duncan, R.; Gaspar, R. Nanomedicine(s) under the microscope. *Mol. Pharmaceutics* **2011**, *8* (6), 2101−41.

(26) Immordino, M. L.; Dosio, F.; Cattel, L. Stealth liposomes: review of the basic science, rationale, and clinical applications, existing and potential. *Int. J. Nanomed.* **2006**, *1* (3), 297−315.

(27) Erdogan, S. Liposomal nanocarriers for tumor imaging. *J. Biomed. Nanotechnol.* **2009**, *5* (2), 141−50.

(28) Cormode, D. P.; Skajaa, T.; Fayad, Z. A.; Mulder, W. J. Nanotechnology in medical imaging: probe design and applications. *Arterioscler., Thromb., Vasc. Biol.* **2009**, *29* (7), 992−1000.

(29) Kelly, C.; Jefferies, C.; Cryan, S. A. Targeted liposomal drug delivery to monocytes and macrophages. *J. Drug Delivery* **2011**, *2011*, 727241.

(30) Almer, G.; Saba-Lepek, M.; Haj-Yahya, S.; Rohde, E.; Strunk, D.; Frohlich, E.; Prassl, R.; Mangge, H. Globular domain of adiponectin: promising target molecule for detection of atherosclerotic lesions. *Biologics* **2011**, *5*, 95−105.

(31) Starcher, B. A ninhydrin-based assay to quantitate the total protein content of tissue samples. *Anal. Biochem.* **2001**, *292* (1), 125−9.

(32) Pali-Scholl, I.; Herzog, R.; Wallmann, J.; Szalai, K.; Brunner, R.; Lukschal, A.; Karagiannis, P.; Diesner, S. C.; Jensen-Jarolim, E. Antacids and dietary supplements with an influence on the gastric pH increase the risk for food sensitization. *Clin. Exp. Allergy* **2010**, *40* (7), 1091−8.

(33) Drew, A. F.; Tipping, P. G. T helper cell infiltration and foam cell proliferation are early events in the development of atherosclerosis in cholesterol-fed rabbits. *Arterioscler., Thromb., Vasc. Biol.* **1995**, *15* (10), 1563−8.

(34) Colombo, M. B.; Haworth, S. E.; Poli, F.; Nocco, A.; Puglisi, G.; Innocente, A.; Serafini, M.; Messa, P.; Scalamogna, M. Luminex technology for anti-HLA antibody screening: evaluation of perform-

ance and of impact on laboratory routine. *Cytometry, Part B* **2007**, *72* (6), 465−71.

(35) Libby, P.; Okamoto, Y.; Rocha, V. Z.; Folco, E. Inflammation in atherosclerosis: transition from theory to practice. *Circ. J.* **2010**, *74* (2), 213−20.

(36) Libby, P.; Nahrendorf, M.; Weissleder, R. Molecular imaging of atherosclerosis: a progress report. *Tex. Heart Inst. J.* **2010**, *37* (3), 324−7.

(37) Nahrendorf, M.; Sosnovik, D. E.; Weissleder, R. MR-optical imaging of cardiovascular molecular targets. *Basic Res. Cardiol.* **2008**, *103* (2), 87−94.

(38) Choudhury, R. P.; Fisher, E. A. Molecular imaging in atherosclerosis, thrombosis, and vascular inflammation. *Arterioscler., Thromb., Vasc. Biol.* **2009**, *29* (7), 983−91.

(39) Pinderski Oslund, L. J.; Hedrick, C. C.; Olvera, T.; Hagenbaugh, A.; Territo, M.; Berliner, J. A.; Fyfe, A. I. Interleukin-10 blocks atherosclerotic events in vitro and in vivo. *Arterioscler., Thromb., Vasc. Biol.* **1999**, *19* (12), 2847−53.

(40) Pinderski, L. J.; Fischbein, M. P.; Subbanagounder, G.; Fishbein, M. C.; Kubo, N.; Cheroutre, H.; Curtiss, L. K.; Berliner, J. A.; Boisvert, W. A. Overexpression of interleukin-10 by activated T lymphocytes inhibits atherosclerosis in LDL receptor-deficient Mice by altering lymphocyte and macrophage phenotypes. *Circ. Res.* **2002**, *90* (10), 1064−71.

(41) Mallat, Z.; Heymes, C.; Ohan, J.; Faggin, E.; Leseche, G.; Tedgui, A. Expression of interleukin-10 in advanced human atherosclerotic plaques: relation to inducible nitric oxide synthase expression and cell death. *Arterioscler., Thromb., Vasc. Biol.* **1999**, *19* (3), 611−6.

(42) Mallat, Z.; Besnard, S.; Duriez, M.; Deleuze, V.; Emmanuel, F.; Bureau, M. F.; Soubrier, F.; Esposito, B.; Duez, H.; Fievet, C.; Staels, B.; Duverger, N.; Scherman, D.; Tedgui, A. Protective role of interleukin-10 in atherosclerosis. *Circ. Res.* **1999**, *85* (8), e17−24.

(43) Nishihira, K.; Imamura, T.; Yamashita, A.; Hatakeyama, K.; Shibata, Y.; Nagatomo, Y.; Date, H.; Kita, T.; Eto, T.; Asada, Y. Increased expression of interleukin-10 in unstable plaque obtained by directional coronary atherectomy. *Eur. Heart J.* **2006**, *27* (14), 1685−9.

(44) Terkeltaub, R. A. IL-10: An "immunologic scalpel" for atherosclerosis? *Arterioscler., Thromb., Vasc. Biol.* **1999**, *19* (12), 2823−5.

(45) Crawley, J. B.; Williams, L. M.; Mander, T.; Brennan, F. M.; Foxwell, B. M. Interleukin-10 stimulation of phosphatidylinositol 3-kinase and p70 S6 kinase is required for the proliferative but not the antiinflammatory effects of the cytokine. *J. Biol. Chem.* **1996**, *271* (27), 16357−62.

(46) Asadullah, K.; Sterry, W.; Volk, H. D. Interleukin-10 therapy—review of a new approach. *Pharmacol. Rev.* **2003**, *55* (2), 241−69.

(47) Tan, J. C.; Indelicato, S. R.; Narula, S. K.; Zavodny, P. J.; Chou, C. C. Characterization of interleukin-10 receptors on human and mouse cells. *J. Biol. Chem.* **1993**, *268* (28), 21053−9.

(48) Abhilash, M. Potential applications of Nanoparticles. *Int. J. Pharma Bio Sci.* **2010**, *1* (1), 12.

(49) Uppal, R.; Caravan, P. Targeted Probes for Cardiovascular MR Imaging. *Future Med. Chem.* **2010**, *2* (3), 451−70.

(50) Voinea, M.; Simionescu, M. Designing of 'intelligent' liposomes for efficient delivery of drugs. *J. Cell. Mol. Med.* **2002**, *6* (4), 465−74.

(51) Helbok, A.; Decristoforo, C.; Dobrozemsky, G.; Rangger, C.; Diederen, E.; Stark, B.; Prassl, R.; von Guggenberg, E. Radiolabeling of lipid-based nanoparticles for diagnostics and therapeutic applications: a comparison using different radiometals. *J. Liposome Res.* **2010**, *20* (3), 219−27.

(52) Frascione, D.; Diwoky, C.; Almer, G.; Opriessnig, P.; Vonach, C.; Gradauer, K.; Leitinger, G.; Mangge, H.; Stollberger, R.; Prassl, R. Ultrasmall superparamagnetic iron oxide (USPIO)-based liposomes as magnetic resonance imaging probes. *Int. J. Nanomed.* **2012**, *7*, 2349−59.

(53) Lauw, F. N.; Pajkrt, D.; Hack, C. E.; Kurimoto, M.; van Deventer, S. J.; van der Poll, T. Proinflammatory effects of IL-10 during human endotoxemia. *J. Immunol.* **2000**, *165* (5), 2783−9.

(54) Ishida, T.; Kiwada, H. Accelerated blood clearance (ABC) phenomenon upon repeated injection of PEGylated liposomes. *Int. J. Pharm.* **2008**, *354* (1−2), 56−62.

(55) Zhou, G.; Ma, Y.; Jia, P.; Guan, Q.; Uzonna, J. E.; Peng, Z. Enhancement of IL-10 bioactivity using an IL-10 peptide-based vaccine exacerbates Leishmania major infection and improves airway inflammation in mice. *Vaccine* **2010**, *28* (7), 1838−46.

(56) Armstrong, L.; Jordan, N.; Millar, A. Interleukin 10 (IL-10) regulation of tumour necrosis factor alpha (TNF-alpha) from human alveolar macrophages and peripheral blood monocytes. *Thorax* **1996**, *51* (2), 143−9.

(57) Almer, G.; Wernig, K.; Saba-Lepek, M.; Haj-Yahya, S.; Rattenberger, J.; Wagner, J.; Gradauer, K.; Frascione, D.; Pabst, G.; Leitinger, G.; Mangge, H.; Zimmer, A.; Prassl, R. Adiponectin-coated nanoparticles for enhanced imaging of atherosclerotic plaques. *Int. J. Nanomed.* **2011**, *6*, 1279−90.